2438 BULLETIN OF THE CHEMICAL SOCIETY OF JAPAN, VOL. 50 (9), 2438—2441 (1977) [Vol. 50, No. 9

The Formation of $VOSO_4$ on the Surface of V_2O_5 in the Oxidation of SO_2 as Studied by ESR

Yoshiya Kera and Keiji Kuwata
Department of Chemistry, Faculty of Science, Osaka University, Toyonaka, Osaka 560

(Received December 27, 1976)

To obtain information on the arrangements of the $VOSO_4$ phase in the surface layer of the V_2O_5 single crystal, the angular dependencies of an asymmetric ESR spectrum which has been found in the crystal under the conditions of SO_2 oxidation and assigned to the $VOSO_4$ phase were examined in detail. Two types of the angular dependency of the spectrum on the static magnetic field were clearly differentiated from each other. In the main spectrum, the direction of $g_{//}$ was completely consistent with the b-axis of the V_2O_5 crystal, while, on the other hand, in the minor spectrum, it took rather random orientations. From comparisons of the crystal structures between V_2O_5 and $VOSO_4$, it was deduced, preliminarily, that the α-$VOSO_4$ phase with a layer structure, was regularly aligned along the layer of the V_2O_5 lattice and that the β-$VOSO_4$ phase without a layer structure took a relatively random orientation to the lattice.

Vanadium oxides, which were promoted with alkali metals and/or supported on silica and alumina gels, have been used as catalysts in the production of sulfuric acid and organic acids. Numerous investigators have attempted to make clear their catalytic properties and reaction mechanisms, especially in SO_2 oxidation.[1] Their results, however, seem to conflict with each other. This is because of some changes in the surface states to which catalysts are subjected in preparation[2] and working.[3] On the other hand, a simple and reversible change in the ESR spectrum was found in the highly purified V_2O_5 single crystal under the conditions of SO_2 oxidation. It was previously reported that, at lower temperatures, the $VOSO_4$ phase existed stably, while at higher temperatures oxygen vacancies remained in the surface layer under the conditions of SO_2 oxidation.[4]

In the present study, in order to obtain information on the structure of the $VOSO_4$ formed in the surface layer of the V_2O_5 crystalline lattice, the angular dependencies of the asymmetric ESR spectrum on the static magnetic field were examined in detail. The growth of $VOSO_4$ in the surface layer of V_2O_5 crystal will be preliminarily discussed.

Experimental

Preparation and Treatment of V_2O_5 Single Crystal. The V_2O_5 powder which was used as the starting material was obtained by the thermal decomposition of NH_4VO_3 (special grade, Wako Pure Chem. Co.) at 600 °C for 3 h in an air stream. The purification of the V_2O_5 powder was carried out chemically according to the procedures reported by McCarley *et al.*[5] The V_2O_5 single crystal was prepared by a zone-melting method in a Pt boat. The crystal was cut out in a size (mm^3) of about $1.4\times0.5\times9$ (wt 0.021 g) and was placed in a quartz tube (4 mm in outer diameter) for the reaction and for ESR measurement. The sample was preliminarily heated at about 500 °C for 1 h under evacuation. After the sample had then cooled to room temperature, a gaseous mixture (SO_2 : air$=37:20$) of 500 mmHg* was introduced and the tube was sealed. The inner volume of the sealed tube was 6 cm^3. The reaction temperature was kept at 617 °C (±1 °C). At time, the reaction tube was taken out from the furnace, and the intensities and line shapes of the ESR spectrum were checked.

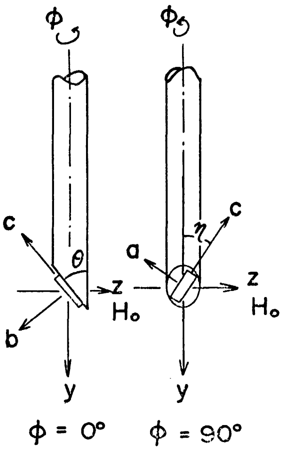

Fig. 1. Rotating operations and relations among crystal axes, experimental coordinates and H_0.

After treatment for 312 h, the crystal was taken out from the reaction tube and was cut out again in a size (mm^3) of about $1.4\times0.3\times4$, in order to measure the angular dependencies of the ESR spectrum.

Rotation Apparatus and Crystal Settings. A quartz rod, the end of which was cut out at a given angle (the angle is denoted as θ) to the rod axis, was mounted on a rotating divice around the vertical axis (the angle of the rotation is denoted as ϕ). In this experiment, six quartz rods, the θ values of which equal 0, 30, 45, 60, and 90° respectively, were used. The accuracy in θ was about 1°. The crystal was placed on the cut plane of the rod at a given angle between the long axis of the elliptical-cut plane of the rod and the c-axis of the crystal (the angle is denoted in η). The relations among the crystal axes and the laboratory coordinates are illustrated in Fig. 1. The three ways of rotation were chosen as follows:

θ: rotation angle around the x-axis (experimental coord.) at $\phi=0°$
ϕ: rotation angle around the y-axis (experimental coord.)
η: rotation angle around the b-axis (crystal axis).

η was determined by use of a micrometerscope (10X) with a graduator; the accuracy was about 1°. ϕ was changed from 0 to 180° at 5° intervals, and accuracy in ϕ was about 0.5°.

ESR Measurements. The ESR measurements were carried out at 77 K by means of a home made X-band spectrometer. The modulation frequency was 455 kHz. The microwave frequency was determined by means of a wave meter,

---

* 1 mmHg$=1.333\times10^2$ Pa.

and the calibration of the magnetic field was done by the use of DPPH and Mn(II) ions doped in MgO. The determination of the concentration of the unpaired electron was done by comparing the integrated intensities with those of a known amount of the $CuSO_4 \cdot 5H_2O$ single crystal. The growth of the spectrum was estimated by comparing the intensities with the DPPH. For the check of the line shape, the spectrum was observed in several different directions of the magnetic field in each measurement.

Results

V_2O_5 Single Crystals Heated in SO_2+Air. No ESR signal was found initially in the V_2O_5 crystal, which was prepared from cautiously purified V_2O_5 powder. The crystal exposed to a gaseous mixture of SO_2 and air at 617 °C for 32 h, however, showed an asymmetric ESR signal. The intensity increased with the time up to about 180 h. The growth of the spectrum with the time is illustrated in Fig. 2. Finally, the spin concentration increased up to about 2×10^{17}. The line shape did not change with the time.

Angular Dependencies of ESR Spectrum. Sharp Signal: When both θ and η are fixed at zero, the change in the spectrum with ϕ is demonstrated in Fig. 3. The figure shows clearly that a strong sharp signal is gradually moving toward a low field as the direction of the magnetic field changes from $H_0//b$ to $H_0//a$ in the ba-plane of the crystal. Besides this, a minor signal, which seems to consist of more than one component, was seen, but the angular behavior is not clear. The sharp signal also behaved similarly when θ was fixed at 0 and at a η of any value from 0 to 90°. When η was fixed at 0° and the θ was of any value between 0 and 90°, the moving range of the sharp component with ϕ was not constant; the larger θ was, the narrower the moving range became. In the limiting case of $\eta=0°$ and a θ value close to 0°, the sharp signal seems always to be at the lowest magnetic field during the change in ϕ, as is demonstrated in Fig. 4. These results for the sharp signal clearly indicate that the $\boldsymbol{g}$-tensor has approximately an axial symmetry, that the direction of $g_{//}$ coincides with the b-axis of the crystal, and that $g_{\perp}$ is in the ac-plane.

The g-values of the sharp signal at each θ are plotted against ϕ in Fig. 5. The full lines are the theoretical one, calculated using the values of $g_{//}=1.924$ and $g_{\perp}=1.970$ obtained by the least-square treatment of the data by the use of the familiar equation, $g^2=g_{//}^2\cos^2\delta+g_{//}^2\sin^2\delta$, where δ denotes the angle between $g_{//}$ and H_0.

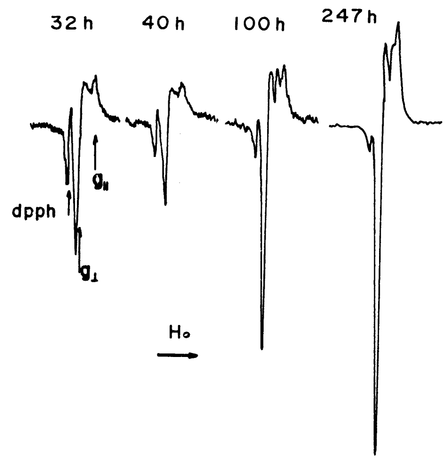

Fig. 2. Change in the intensity of ESR spectrum in V_2O_5 single crystal during SO_2 oxidation reaction.

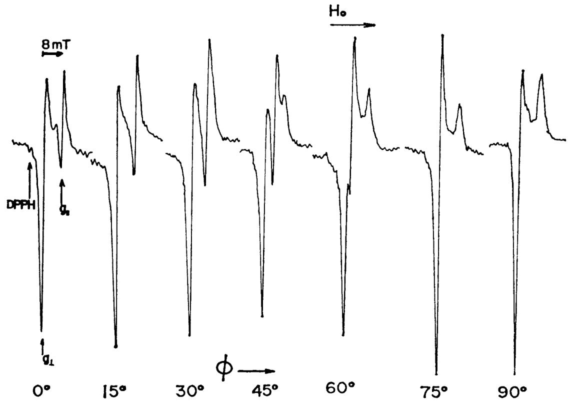

Fig. 3. Change in ESR spectrum with change in the direction of H_0 in the crystal ab-plane from $H_0//b$ to $H_0//a$.

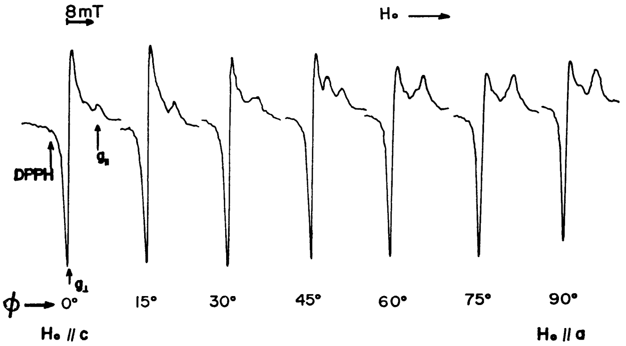

Fig. 4. Change in ESR spectrum with the change in the direction of H_0 in the crystal ac-plane from $H_0//c$ to $H_0//a$.

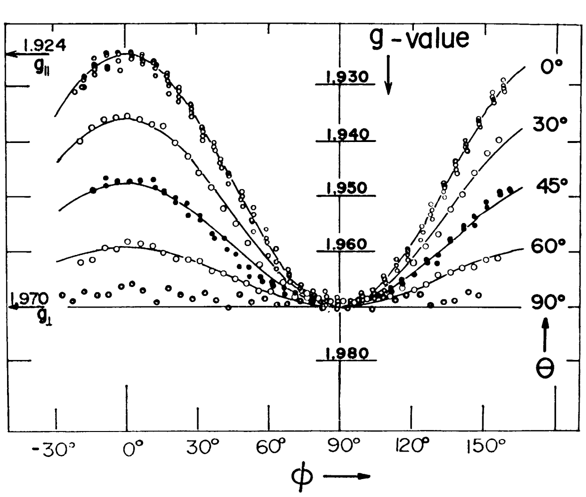

Fig. 5. Angular dependency of the sharp signal on θ. Figure shows following cases: at $\theta=0°$ with $\eta=0$, 30, 45, 60, and 90°; at $\theta=45°$ with at $\eta=0$ and 45°; and with $\theta=30$, 60, and 90° only at $\eta=0°$.

In the case of $\theta=0°$, at η values of 0, 30, 45, 60, and 90°, and in the case of $\theta=45°$, at η values of 0° and 45°, the results are given together. In the other cases, only results at $\eta=0°$ are given. Except in the case of $\theta=90°$, the g-values concentrate close to the theoretical curves. The fluctuations of the g-values in the case of $\theta=90°$ seem to due to the overlap of some minor components, as will be discussed below.

Other Minor Signals: It may be seen in Fig. 4 that the other minor signals in the spectrum move from a low to a high field with the change in the direction of the H_0 in the ac-plane from $H_0//c$ to $H_0//a$. As several components overlap complicatedly and seem to move independently of each other, the centers of the groups of these signals can not be preciesly determined. In the case of $\theta=90°$ and $\phi=0°$, however, the g-values estimated from the distances between the center of the group and that of DPPH can be plotted against ϕ, as is shown in Fig. 6. A periodical change is seen, especially near the maximum point in the figure. The dotted lines are the theoretical ones, calculated by the use of the same equation and parameters as those used in the case of the sharp signal. To obtain a good fit, several directions of g were tried parallel to the a- and c- axes and deviating by ±45° from the axes in the ac-plane; the best fit was thus obtained. It may be seen in the figure that there are also other groups of points which are not distributed on any of the dotted lines. This may indicate that there are other components which have $g_{//}$ components out of the ac-plane. Nearly the same periodicities as in the case of the H_0 change in the ac-plane (*cf.* Fig. 6) were also seen near the c- and a-axes in the case of the H_0 variations in the ab- and bc-planes of the V_2O_5 crystal. However, the minor signals can not be determined practically because they are extensively disturbed by the sharp signal.

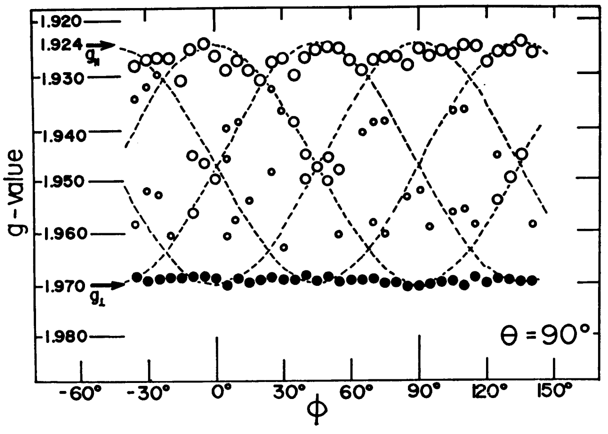

Fig. 6. Angular variations of the minor signal with the change in H_0 in the ac-plane. Dotted lines denote the theoretical calculations under the assumptions that $g_{//}$ is in the ac-plane and is parallel to a-, c-axis and the axes deviated by ±45° from a- or c-axis. Closed circles denote the values of the sharp signal. Large open circles denote the values of relatively clear signal and the small circles that of not so clear signal.

Discussion

Possible Structures of the $VOSO_4$ Formed in the V_2O_5 Crystal in the Oxidation of SO_2 with Air. Many investigators have found several types of ESR spectra in the V_2O_5 crystal, in some cases by the addition of metal impurities.[6-10] The results have always indicated that the direction of $g_{//}$ coincides with the b-axis, and the spectra show hfs due to V (IV) ions which are diluted inside the V_2O_5 lattice and are sufficiently isolated from each other. Therefore, the sharp and asymmetric spectrum in the present study can not be ascribed to these species. On the other hand, the possibilities of ascribing this ESR spectrum to some lower vanadium oxide compounds (*e.g.*, V_3O_7, V_6O_{13}, and VO_2) can also be excluded. On the contrary, existence of the $VOSO_4$ phase has been strongly supported by previous study.[4]

Two types of crystal structures have been reported in $VOSO_4$:[11] the α-form (tetragonal) and the β-form (orthorhombic). The α-form has the layer structure shown in Fig. 7,[12] and the vanadium-oxygen bond (V=O) takes only one direction, which coincides with the c-axis in the crystal. In the β-form, the layer structure is completely destroyed, as is shown schematically in Fig. 8.[13] The vanadium-oxygen bond (V=O) takes two directions deviating by about ±22° from the a-

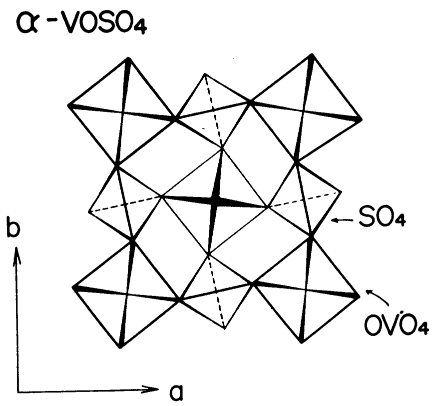

Fig. 7. A schematic representation of α-$VOSO_4$ crystal structure by Ladwig.[12] A layer structure is kept, although crystal coordinate differ from that in V_2O_5.

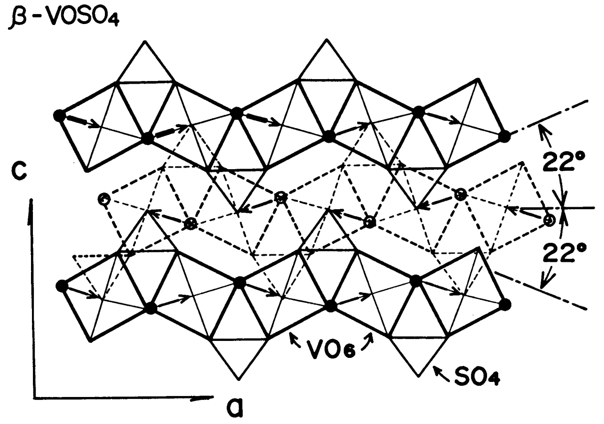

Fig. 8. A schematic representation of the crystal structure of β-$VOSO_4$ by Kierkegaard *et al.*[13]

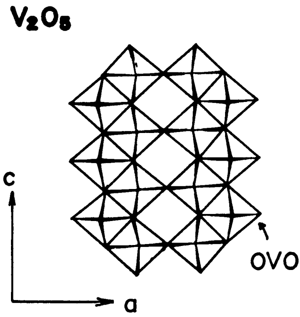

Fig. 9. A schematic representation of V_2O_5 crystal structure by Byström *et al.*[14)] and Bachmann *et al.*[15)] Construction of a sheet from zig-zag double chains.

axis on the ac-plane of the crystal. On the other hand, V_2O_5 is orthorhombic (Pnmn) and has a layer structure, as is shown in Fig. 9.[14,15)] All the V=O bonds are alined on a straight line, which is parallel to the b-axis.

α-$VOSO_4$ in the crystalline state could be realized from the V_2O_5 crystal, keeping the layer structure in such a manner that the oxygen ions in the four corners of the VO_5 square-pyramid unit of V_2O_5 are simply replaced by the oxygen atoms of the four SO_4^{2-} tetrahedrons. On the other hand, in the β-$VOSO_4$ the same replacement of the oxygen of the VO_5 unit by the oxygen of SO_4^{2-} could occur only after the destruction of the layer structure. Therefore, we can expect that the growth of the α-phase in the V_2O_5 crystal occurs more easily than that of the β-phase.

Arrangement of the $VOSO_4$ Phases in the V_2O_5 Lattice under the SO_2 Oxidation. The directions of the V=O bond, which are coincident with the $g_{//}$ of the $\boldsymbol{g}$-tensor in these crystals, may be clearly summarized as follows: in V_2O_5 and α-$VOSO_4$, it takes only one direction, parallel to the b-axis, but in β-$VOSO_4$, a pair of directions, deviating from the a-axis by about ±22° on the ac-plane. The $\boldsymbol{g}$-tensor should have the same value in both α- and β-$VOSO_4$ because they have the same local field around the vanadyl ion.

The alignments of the V=O bond and principal axes of the $\boldsymbol{g}$-tensor in the $VOSO_4$ crystal can be primarily known from the crystal structure. By connecting the crystal structures with the results of the $\boldsymbol{g}$-tensor analysis, therefore, the possible arrangements of $VOSO_4$ phase in the V_2O_5 lattice can be discussed.

The finding that the axis for the $g_{//}$ of the sharp signal in the spectrum was completely coincident with the b-axis of the V_2O_5 crystal strongly suggests that the $VOSO_4$ formed in the V_2O_5 lattice is the α-form. Both α-$VOSO_4$ and V_2O_5 have the same layer structure, except only for such differences that the oxygen atoms in the four corners of the VO_5 square-pyramid in V_2O_5 are replaced by the oxygen atoms of the SO_4^{2-} tetrahedron in α-$VOSO_4$. The change from V_2O_5 to α-$VOSO_4$ seems to be possible in the crystalline states in such a manner that the oxygen atoms in the four corners of the VO_5 square-pyramidal unit in V_2O_5 are simply replaced by the oxygen atoms of the four SO_4^{2-} tetrahedrons; then the layer structure and the direction of V=O bonds are kept unchanged in the α-$VOSO_4$ lattice.

In the case of the minor components of the spectrum, as has been preliminarily described above, the axis for $g_{//}$ exists on the ac-plane and on the other planes as a pair of $\boldsymbol{g}$-tensors, which take an angle of about 45° toward each other. From the correspondence of the directions of the $\boldsymbol{g}$-tensor with that of the V=O bond in β-$VOSO_4$, the minor components can possibly be ascribed to β-$VOSO_4$. Besides, the possibility of the growth of α-$VOSO_4$ on dislocation or some other imperfection of the crystal can not, of cause, be ruled out.

It can reasonably be expected that a clear-cut and reversible transformation between the formation and decomposition of the $VOSO_4$ phase in the V_2O_5 crystalline lattice occurs more favorably in the case of the α-$VOSO_4$ than the β-$VOSO_4$ phase. The fact that a surface brilliance always remained after repetitions of the formation and the decomposition of the $VOSO_4$ phase in the V_2O_5 lattice[4)] also suggests strongly that, in the cleaven plane (the ac-plane) of the V_2O_5, α-$VOSO_4$ phase easily grows with a topochemical relation. From this suggestion, the important role of the ac-plane in catalysis can be understood in the case of SO_2 oxidation as well as in the case of CO oxidation.[16)]

References

1) For instance (a) P. Mars and J. G. H. Maessen, *Proc. Int. Congr. Catal. 3rd, Amsterdom*, **1**, 266 (1964); *J. Catal.*, **10**, 1 (1968); (b) G. K. Boreskov, R. A. Buyanov, and A. A. Ivanov. *Kinet. Katal.*, **8**, 153 (1967); G. K. Boreskova, L. P. Davydova, V. M. Mastikhin, and G. M. Polyakova, *Dokl. Akad. Nauk. SSSR*, **210**, 626 (1973); (c) A. R. Glueck and C. N. Kenney, *Chem. Eng. Sci.*, **23**, 1257 (1968).

2) H. Tanaka and A. Matsumoto, *Bull. Chem. Soc. Jpn.*, **39**, 874 (1966).

3) G. K. Boreskov, L. P. Davydova, V. M. Mastikhin, and G. M. Polyakova, *Dokl. Akad. Nauk. SSSR*, **171**, 648 (1966); V. M. Mastikhin, G. M. Polyakova, Ya. Zyulkovskii, and G. K. Boreskov, *Kinet. Katal.*, **11**, 1463 (1970).

4) Y. Kera and K. Kuwata, *Bull. Chem. Soc. Jpn.*, to be submitted.

5) R. E. McCarley and J. W. Roddy, *J. Less-Common Met.* **2**, 29 (1960); J. Haemers, *Bull. Soc. Chim. Belg.* **79**, 473 (1970).

6) J. L. Ragle, *J. Chem. Phys.* **38**, 2020 (1963).

7) V. A. Ioffe and I. B. Patrina, *Soviet Phys. -Solid State*, **6**, 2425 (1964); *ibid.*, **10**, 639 (1968).

8) E. Gilis and E. Boesman, *Phys. Status Solidi*, **14**, 337, 349 (1966).

9) K. Hirota, K. Kuwata, and Y. Kera, *Bull. Chem. Soc. Jpn.*, **43**, 3017 (1970).

10) G. Sperlich, *Z. Phys.*, **250**, 335 (1972).

11) J. Selbin, *Chem. Rev.*, **65**, 153 (1965).

12) V. G. Ladwig, *Z. Anorg. Allg. Chem.*, **364**, 225 (1969).

13) P. Kierkegaard and J. M. Longo, *Acta Chem. Scand.*, **19**, 1905 (1965).

14) A. Byström, K. A. Wilhelmi, and O. Brotzen, *Acta Chem. Scand.*, **4**, 1119 (1950).

15) H. G. Bachmann, F. R. Ahmed, and W. H. Barnes, *Z. Kristallogr.*, **115**, 110 (1961).

16) K. Hirota, Y. Kera, and S. Teratani, *J. Phys. Chem.*, **72**, 3133 (1968); Y. Kera, K. Hirota, *ibid.*, **73**, 3973 (1969).